Nigerian Research Journal of Engineering and Environmental Sciences 7(1) 2022 pp. 178-191
p ISSN: 2635-3342; e ISSN: 2635-3350

Nigerian Research Journal of Engineering and Environmental Sciences
Journal homepage: www.rjees.com

Original Research Article

Bending Analysis of a Three-Dimensional Isotropic Thick Plate using Energy Method with Trigonometric Displacement Functions

***[1]Onyeka, F.C., [2]Nwa-David, C.D. and [1]Sule, J.**

[1]Department of Civil Engineering, Edo State University, Uzairue, Edo State, Nigeria.
[2]Department of Civil Engineering, Michael Okpara University of Agriculture, Umudike, Abia State, Nigeria.
*onyeka.festus@edouniversity.edu.ng; nwadavid.chidobere@mouau.edu.ng

http://doi.org/10.5281/zenodo.6724573

ARTICLE INFORMATION

Article history:
Received 22 Apr, 2022
Revised 04 Jun, 2022
Accepted 04 Jun, 2022
Available online 30 Jun, 2022

Keywords:
Exact bending analysis
3-D plate theory
Isotropic thick plate
Energy method
Trigonometric displacement function

ABSTRACT

This paper applied a trigonometric function to the study of exact bending analysis of a three-dimensional isotropic rectangular thick plate that is clamped at the first-three edges and the other edge simply supported (CCCS). This function was developed by making use of the three-dimensional (3-D) static theory of elasticity which consist of entire stress components used in the total potential energy equation formulation. The compatibility equation which was built from the energy equation transformation which was used to get the slope and deflection relationship. The solution of compatibility equation gave rise to the exact trigonometric deflection function while the coefficient of deflection of the plate was obtained from the governing equation through direct variation method. These solutions were applied in the analysis of the bending problem of the CCCS rectangular plate by establishing the formula for calculating the displacement and stresses of the plate. The result of this study showed that the value of the deflection and stresses decrease as the span-thickness ratio increases. The comparative study shows that the present study differs with classical plate theory (CPT) and refined plate theory (RPT) of assumed deflection by 5.6% and 4.9% respectively, whereas it differs from the exact 2-D RPT by 3.7%. This showed that the 3-D plate theory is a sufficient model for the plate analysis, which produced an exact solution to the bending problem of any category of rectangular plate under CCCS boundary condition.

1. INTRODUCTION

Plates are basically three-dimensional structural materials with extensive application in engineering structures such as offshore platform structures, ship hulls and decks, aircraft wings, railways, roof, floor

slabs, and spacecraft panels (Onyeka *et al*., 2021a, b). Based on shapes, plates can be classified as skew, quadrilateral, elliptical, square, circular or rectangular. Also, according to their constituent materials, they may also be classified as anisotropic, orthotropic, isotropic, homogeneous, and non-homogeneous (Osadebe *et al.,* 2016; Onyeka *et al*., 2021c). Plate materials are of different support conditions such as simply supported, free and fixed conditions. Plates are mostly classified as thin, moderately thick or thick plates based on their thickness (Chandrashekhara, 2001; Onyeka *et al*., 2022a). Generally, the thickness of a thin plate is lesser than that of thick plate. Unlike thin plates, the straight line in thick plates at right angle to the middle surface before elongation does not remain the same after deformation. In engineering, thick plates have attracted more research attention as their application is numerous due to their distinctive structural features such their tailored structural properties, economical attractiveness, light weight and their ability to withstand heavy loads (Onyeka, and Mama, 2021; Onyeka, 2021; Onyeka *et al*., 2022b).

The plate's deformation at right angles to the plate surface due to the impact of forces and moments is known as Bending (Onyeka and Okeke, 2021a; Gujar and Ladhane, 2015). Due to the applied load, a structural member is displaced and stresses are induced. Plates can be subjected to transverse or uniformly distributed loads at the plate's middle plane. A plate is under uniformly distributed lateral load when it is subjected to an applied load at the boundary perpendicular to the mid-surface and distributed through its thickness. Plates can bend or elastically become deformed as a result of such lateral loading (Onyeka, 2020; Onyeka, and Okeke, 2021b). Such deformation can lead to a structural failure if not properly handled. To ensure the safety of thick plates for resisting design load, bending analysis is essential so as to determine the displacements, moments and stresses at various points of the plate.

Researches on plate analysis consists of vibration, buckling and bending (Reddy, 2006). To study the bending characteristics of plates, several theories have been employed such as the classical plate theory (CPT) and the refined plate theories (RPT) which include the first order shear deformation theory (FSDT) and the higher-order shear deformation plate theory (HSDT). The classical plate theory, also known as the Kirchhoff plate theory (Kirchhoff, 1850) is mainly applied in thin plate analysis as it cannot evaluate the exact bending behavior of thick plates because of the neglected shear deformation effect (Mama, 2017). The RPT which is used for thick plate analysis addressed the effect of transverse shear deformation during analysis but with a shear correction factor to account for it in FSDT (Reissner, 1945; Mindlin, 1951) and with variation of transverse shear stress from top to bottom of the plate in HSDT using different functions (Onyeka and Okeke, 2021c; Onyeka *et al*., 2021d; Sayyad, 2013). Since these theories neglected normal strain and stress along the thickness axis of the plate, they are regarded as an incomplete 3-D plate theory. The analysis of plates as two-dimensional (2-D) element among researchers and the construction industry has often led to inaccurate and unreliable design as plates are basically three-dimensional structural elements and ought to be analyzed three-dimensionally (Onyeka and Okeke, 2022c).

Ike (2017) investigated the bending behavior of CSSS rectangular Kirchhoff plates using Kantorovich-Galerkin method. The author derived deflection and bending moment coefficients for deflection at the center of the plates under uniform load using one term Kantorovich-Galerkin solution without carrying out the critical lateral load analysis. The stresses in the direction of thickness axis were not considered neither was plated with the CCCS boundary condition taken into account. 3-D plate theory with energy approach and trigonometric function were not employed. Nwoji *et al.* (2018) used the Ritz method to analyze the plate bending problem of a rectangular SSSS Kirchhoff plate. Exact solutions were obtained as exact shape functions were used and the method employed by the authors gave identical results compared with those with the Navier double Fourier sine series method. The authors did not consider a thick plate as their assumption is restricted to CPT which cannot give a good outcome for a relatively thick plate. Their study failed to cover CCCS plate support conditions. Onyeka *et al.* (2020) developed a new model for the evaluation of the plate's critical lateral imposed load and the polynomial shear deformation theory was used to study the influence of aspect ratio, shear and deflection on the critical lateral load of the plates. Although the outcome of their study revealed that the direct variational method circumvents the tedious and rigorous procedures involved in the classical and numerical methods, their study failed to cover 3-D plates with CCCS

boundary conditions using trigonometric functions. Ibearugbulem *et al.* (2018) determined the displacements and stresses of all-round-clamped rectangular thick plate of various span-to-depth ratio using polynomial function in a variational method. Although the authors did not apply any shear correction factor and the zero shear stress condition on the upper and lower surfaces of the plate were satisfied; they failed to consider all the stresses in the plate and plates with the CCCS edge condition were not addressed. Onyeka and Ibearugbulem (2020) applied nonlinear strain-displacement polynomial shape function with a direct energy method to get closed-form bending solutions of CCCC and CCFC thick rectangular plates. The authors obtained the governing equations that solved the deflection problem of the plates using the principle of variational calculus. The effects of aspect ratio of the critical lateral load were investigated in their study. The authors failed to consider the displacement and stresses and 3-D plate theory was not employed neither did the authors apply trigonometric shape function. Their study failed to cover plates with CCCS boundary conditions. Sayyad and Ghugal (2012) used refined theory of shear deformation with exponential functions to analyze displacement and stresses for thick plates with simply supported edges. The outcome of their analysis was satisfactory compared with other refined plate theories. However, their study failed to apply trigonometric displacement function with energy method and a three-dimensional thick plate with three clamped and one simply supported edge condition was not covered. Onyeka *et al.* (2021c) analyzed and presented the bending of plates with free support at the third edge and the other three edges simply supported (SSFS) under uniform distributed transverse loads, applying 2-D theory with polynomial displacement function. The authors determined the critical load used in predicting the plate's flexural characteristics and the effect of deflection and shear stress on the plate. Their study did not cover CCCS plates. The authors failed to consider the plate stresses neither was trigonometric functions and 3-D plate theory employed. With direct variational method, Onyeka and Edozie (2020) applied RPT of third order to obtain the in-plane displacements, deflections, shear force, bending moments and shear deformation rotations at arbitrary points on rectangular plates with and plates with three clamped edges and one simply supported edge (CCCS). The authors actually studied CCCS edge conditions using polynomial displacement function without considering trigonometric functions which produce a close form solution. Their study did not consider a typical three-dimensional bending analysis of the plate. Ibearugbulem *et al.* (2021) analytically presented a 3-D bending analysis of a thick all-round simply supported plate. The authors used third order shear deformation theory with six strain and stress components to obtain the total potential energy function. The rotations and deflection expression were derived from the solutions of compatibility equations that were obtained by minimizing the function with respect to shear deformation rotations. Although the values of the deflections and stresses obtained from their study were coarse compared with those of refined plate theories, trigonometric functions in an energy approach was not taken into account neither was CCCS plates considered. An alternative I-refined plate theory based on the 3-D formulation was employed by Onyeka and Okeke (2021d), to obtain the exact displacement and stress solutions of the plate with one free support and three clamped boundary conditions (CCFC) with uniformly distributed transverse load using trigonometric displacement functions and the general variation approach. The authors failed to address CCCS plates. On account of three-dimensional theory of elasticity with the numerical approach, Grigorenko *et al.* (2013) obtained the bending solutions of thick plates with clamped edge conditions. Two of the coordinate directions of spline collocation was used by the authors and the displacements and stresses were satisfactory. Although Onyeka and Mama (2021) presented a study with energy method and trigonometric function in their bending analysis, both authors failed to apply the energy method which is more simplified, neither did they address plates with CCCS support conditions.

The assumption that the normal stress and strain along the thickness axis of the plate is negligible, makes these refined plate theories inconsistent and it is regarded as a 2-D plate theory. However, very few scholars employed the 3-D plate theory in their rectangular thick plate bending analysis as shown in the studies reviewed. This study is a plus on thick plate bending analysis using 3-D plate theory as it proves the only sufficient model for the plate analysis which produced an exact solution to the bending problem of any category of rectangular plate under CCCS boundary condition.

The distinctiveness of this work compared to previous works is seen its analytical approach, type of shape functions applied and the plates support conditions. Most of the past studies did not employ energy methods and a thick 3-D plate with three clamped edges and one simply supported boundary conditions were not addressed. To fill this literature gap, this study is worth doing as they focused on analyzing the bending behavior of a CCCS rectangular plate under uniformly distributed transverse load using 3-D plate theory and developing the exact trigonometric displacement function for the analysis by applying the principles of variational calculus.

2. METHODOLOGY

2.1. Kinematics/Constitutive Relationships

By considering a rectangular plate subjected to uniformly distributed load as shown in Figure 1 the displacement-strain relationship was established applying a consideration non-linear deformation of the plate section as presented.

The constitutive equations for five stress components are:

$$u = \frac{zdw}{dy} + z.\theta_x \tag{1}$$

$$v = \frac{zdw}{dy} + z.\theta_y \tag{2}$$

Where u, v, w, θ are the displacement in x, y and z axis, shear deformation slope of the thick rectangular section of plate

$$\varepsilon_x = \frac{\partial u}{\partial x} \tag{3}$$

$$\varepsilon_y = \frac{dv}{\partial y} \tag{4}$$

$$\varepsilon_z = \frac{\partial w}{\partial z} \tag{5}$$

$$\sigma_x = E\left[\left(-\frac{z\partial^2 w}{dx^2} + \frac{F\partial\theta_x}{\partial x}\right) - \mu\left(\frac{z\partial^2 w}{dy^2} + \frac{F\partial\theta_y}{\partial y}\right)\right]/(1-\mu^2) \tag{6}$$

$$\sigma_y = E\left[\left(-\frac{z\partial^2 w}{dy^2} + \frac{F\partial\theta_x}{\partial x}\right) - \mu\left(\frac{z\partial^2 w}{\partial x^2} + \frac{F\partial\theta_y}{\partial y}\right)\right]/(1-\mu^2) \tag{7}$$

$$\tau_{xy} = 2G\left[-\frac{z\partial^2 w}{\partial x\partial y} + F\left(\frac{\partial\theta_x}{dy} + \frac{\partial\theta_y}{dx}\right)\right] \tag{8}$$

$$\tau_{xz} = 2G\left[\frac{z\partial^2 w}{\partial x\partial z} + F\left(\frac{d\theta_x}{\partial z} + \frac{\partial\theta_z}{\partial x}\right)\right] \tag{9}$$

$$\tau_{yz} = 2G\left[\frac{z\partial^2 w}{\partial y\partial z} + F\left(\frac{\partial\theta_y}{\partial z} + \frac{\partial\theta_z}{\partial y}\right)\right] \tag{10}$$

$$G = \frac{E(1-\mu)}{2(1-\mu^2)} \tag{11}$$

Where ε_x, ε_y, ε_z denote normal strain in x, y and z axis, σ_x, σ_y and σ_z denote stress normal to x, y and z axis, τ_{xy}, τ_{xz} and τ_{yz} denote shear stress along x-y, x-z and y-z axis, μ denotes poison ratio and E denotes modulus of elasticity of the plate

Taking the non-dimensional form of coordinates to be R = x/a, Q = y/b and S = z/t corresponding to x, y and z-axes respectively, the six stress components in terms of non-dimensional coordinates are written as:

$$\sigma_x = \frac{Ets}{(1+\mu)(1-2\mu)a}\left[(1-\mu).\frac{\partial\theta_x}{\partial R}+\frac{\mu}{\beta}.\frac{\partial\theta_y}{\partial Q}+\frac{\mu a}{st^2}.\frac{\partial w}{\partial S}\right] \tag{12}$$

$$\sigma_y = \frac{Ets}{(1+\mu)(1-2\mu)a}\left[\mu.\frac{\partial\theta_x}{\partial R}+\frac{(1-\mu)}{\beta}.\frac{\partial\theta_y}{\partial Q}+\frac{\mu a}{st^2}.\frac{\partial w}{\partial S}\right] \tag{13}$$

$$\sigma_z = \frac{Ets}{(1+\mu)(1-2\mu)a}\left[\mu.\frac{\partial\theta_x}{\partial R}+\frac{\mu}{\beta}.\frac{\partial\theta_y}{\partial Q}+\frac{(1-\mu)a}{st^2}.\frac{\partial w}{\partial S}\right] \tag{14}$$

$$\tau_{xy} = \frac{E(1-2\mu)ts}{2(1+\mu)(1-2\mu)a}.\left[\frac{1}{\beta}\frac{\partial\theta_x}{\partial Q}+\frac{\partial\theta_y}{\partial R}\right] \tag{15}$$

$$\tau_{xz} = \frac{E(1-2\mu)ts}{2(1+\mu)(1-2\mu)a}.\left[\frac{a}{ts}\theta_x+\frac{1}{ts}\frac{\partial w}{\partial R}\right] \tag{16}$$

$$\tau_{yz} = \frac{E(1-2\mu)ts}{2(1+\mu)(1-2\mu)a}.\left[\frac{a}{ts}\theta_y+\frac{1}{\beta ts}\frac{\partial w}{\partial Q}\right] \tag{17}$$

Given that: $\beta = \frac{a}{t}$

2.2. Potential Energy Expressions

Total energy expression being the algebraic summation of strain energy (M) and external work (V) is expressed mathematically as:

$$\prod = \mathrm{M} - \mathrm{E} \tag{18}$$

The strain energy equation which is the dot product of stresses and strain as obtained in Equations (3) to (17) is presented in the Equation (19) as:

$$M = \frac{abt}{2}\int_0^1\int_0^1\int_{-0.5}^{0.5}\left(\sigma_x\varepsilon_x+\sigma_y\varepsilon_y+\sigma_z\varepsilon_z+\tau_{xy}\gamma_{xy}+\tau_{xz}\gamma_{xz}+\tau_{yz}\gamma_{yz}\right)dR\,dQ\,dS \tag{19}$$

The potential energy for the plate with uniformly distributed load is given as:

$$E = abq\int_0^1\int_0^1 w\,dR\,dQ \tag{20}$$

Where, the symbol γ_{xy}, γ_{xz} and γ_{yz} denote shear strain along x-y, x-z and y-z axis of the plate, while q, a, b and t denote the uniformly distributed load, length, breadth and thickness of the plate

Thus, putting Equations (19) and (20) into Equation (18) after substituting Equation to (17) into (19) gives:

$$\Pi = \frac{D^* ab}{2a^2}\int_0^1\int_0^1\left[(1-\mu)\left(\frac{\partial\theta_{sx}}{\partial R}\right)^2 + \frac{1}{\beta}\frac{\partial\theta_{sx}}{\partial R}.\frac{\partial\theta_{sy}}{\partial Q} + \frac{(1-\mu)}{\beta^2}\left(\frac{\partial\theta_{sy}}{\partial Q}\right)^2 + \frac{(1-2\mu)}{2\beta^2}\left(\frac{\partial\theta_{sx}}{\partial Q}\right)^2 + \frac{(1-2\mu)}{2}\left(\frac{\partial\theta_{sy}}{\partial R}\right)^2 + \frac{6(1-2\mu)}{t^2}\left(a^2{\theta_{sx}}^2 + a^2{\theta_{sy}}^2 + \left(\frac{\partial w}{\partial R}\right)^2 + \frac{1}{\beta^2}\left(\frac{\partial w}{\partial Q}\right)^2 + 2a.\theta_{sx}\frac{\partial w}{\partial R} + \frac{2a.\theta_{sy}}{\beta}\frac{\partial w}{\partial Q}\right) + \frac{(1-\mu)a^2}{t^4}\left(\frac{\partial w}{\partial S}\right)^2 - \frac{2qa^4 w}{D^*}\right] dR\, dQ \quad (21)$$

2.3. Governing Energy Equation

The solution of the general governing equation is obtained in line with work of Onyeka, *et al.* (2022b) to get the exact deflection equation and slope at x and y axis of the plate as presented in Equations (22), (23) and (24) respectively.

$$w = \Delta_0[1 \quad R \quad Cos\,(c_1R) \;\; Sin\,(c_1R)]\begin{bmatrix}a_0\\a_1\\a_2\\a_3\end{bmatrix}.[1 \quad Q \quad Cos\,(c_1Q) \;\; Sin\,(c_1Q)]\begin{bmatrix}b_0\\b_1\\b_2\\b_3\end{bmatrix} \quad (22)$$

$$\theta_x = \frac{c}{a}.\Delta_0.[1 \quad c_1Sin\,(c_1R) \;\; c_1Cos\,(c_1R)]\begin{bmatrix}a_1\\a_2\\a_3\end{bmatrix}.[1 \quad Q \quad Cos\,(c_1Q) \;\; Sin\,(c_1Q)]\begin{bmatrix}b_0\\b_1\\b_2\\b_3\end{bmatrix} \quad (23)$$

$$\theta_y = \frac{c}{a\beta}.\Delta_0.[1 \quad R \quad Cos\,(c_1R) \;\; Sin\,(c_1R)]\begin{bmatrix}a_0\\a_1\\a_2\\a_3\end{bmatrix}.[1 \quad c_1Sin\,(c_1Q) \;\; c_1Cos\,(c_1Q)]\begin{bmatrix}b_1\\b_2\\b_3\end{bmatrix} \quad (24)$$

Let:

$$w = C_1.h \quad (25)$$

$$\theta_x = \left[\frac{dh}{dR}\right]\left[\frac{C_2}{a}\right] \quad (26)$$

And:

$$\theta_y = \left[\frac{dh}{dQ}\right]\left[\frac{C_3}{a\beta}\right] \quad (27)$$

Where $h, C_1, C_2\ and\ C_3$ is the plate shape function, coefficient of deflection, coefficient of shear deformation along x axis and coefficient of shear deformation along y axis respectively.

The solution of the direct governing equation was obtained by differentiating the total potential energy with respect to the coefficient of deflection (C_1), coefficient of shear deformation with respect to x-axis (C_2) and coefficient of shear deformation with respect to y-axis (C_3) as presented mathematically as:

$$\frac{\partial\Pi}{\partial C_1} = \frac{\partial\Pi}{\partial C_2} = \frac{\partial\Pi}{\partial C_3} = 0 \quad (28)$$

The solution of the governing equation was achieved by differentiation Equation (21) with respect to C_1, C_2, and C_3 to get:

$$\begin{aligned} \Pi = \frac{D^* ab}{2a^4}\Bigg[&(1-\mu){C_2}^2 k_x + \frac{1}{\beta^2}\left[C_2.C_3 + \frac{(1-2\mu){C_2}^2}{2} + \frac{(1-2\mu){C_3}^2}{2}\right]k_{xy} \\ &+ \frac{(1-\mu){C_3}^2}{\beta^4}k_y \\ &+ 6(1-2\mu)\left(\frac{a}{t}\right)^2\left(\left[{C_2}^2 + {C_1}^2 + 2C_1C_2\right].k_z\right. \\ &\left.+ \frac{1}{\beta^2}.\left[{C_3}^2 + {C_1}^2 + 2C_1C_3\right].k_{2z}\right) - \frac{2qa^4k_hC_1}{D^*}\Bigg] \end{aligned} \tag{29}$$

Where:

$$k_x = \int_0^1\int_0^1 \left(\frac{\partial^2 h}{\partial R^2}\right)^2 dRdQ \tag{30}$$

$$k_{xy} = \int_0^1\int_0^1 \left(\frac{\partial^2 h}{\partial R\partial Q}\right)^2 dRdQ \tag{31}$$

$$k_h = \int_0^1\int_0^1 h\,.dRdQ \tag{32}$$

$$k_y = \int_0^1\int_0^1 \left(\frac{\partial^2 h}{\partial Q^2}\right)^2 dRdQ \tag{33}$$

$$k_z = \int_0^1\int_0^1 \left(\frac{\partial h}{\partial R}\right)^2 dRdQ \tag{34}$$

$$k_{2z} = \int_0^1\int_0^1 \left(\frac{\partial h}{\partial Q}\right)^2 dRdQ \tag{35}$$

Minimizing Equation 21 with respect to C_2 and simplifying the outcome gives:

$$\begin{aligned} &\left[(1-\mu)k_x + \frac{1}{2\beta^2}(1-2\mu)k_{xy} + 6(1-2\mu)\left(\frac{a}{t}\right)^2 k_z\right]C_2 + \left[\frac{1}{2\beta^2}k_{xy}\right]C_3 \\ &= \left[-6(1-2\mu)\left(\frac{a}{t}\right)^2 k_z\right]C_1 \end{aligned} \tag{36}$$

Minimizing Equation (21) with respect to C_3 and simplifying the outcome gives:

$$\begin{aligned} &\left[\frac{1}{2\beta^2}k_{xy}\right]C_2 + \left[\frac{(1-\mu)}{\beta^4}k_y + \frac{1}{2\beta^2}(1-2\mu)k_{xy} + \frac{6}{\beta^2}(1-2\mu)\left(\frac{a}{t}\right)^2 k_{2z}\right]C_3 \\ &= \left[-\frac{6}{\beta^2}(1-2\mu)\left(\frac{a}{t}\right)^2 k_Q\right]C_1 \end{aligned} \tag{37}$$

Equations (38) and (39) are the solutions to Equations 36 and 37 respectively:

$$C_2 = AC_1 \tag{38}$$

$$C_3 = BC_1 \tag{39}$$

Minimizing Equation (33) with respect to C_1 and simplifying the outcome gives:

$$6(1-2\mu)\left(\frac{a}{t}\right)^2\left([C_1 + C_1A].k_z + \frac{1}{\beta^2}.[C_1 + C_1B].k_{2z}\right) - \frac{qa^4k_h}{D^*} = 0 \tag{40}$$

Factorizing Equation (40) and simplifying further gives:

$$6(1-2\mu)\left(\frac{a}{t}\right)^2 C_1\left([1 + A].k_z + \frac{1}{\beta^2}.[1 + B].k_{2z}\right) = \frac{qa^4k_h}{D^*} \tag{41}$$

Thus:

$$A_1 = \frac{qa^4}{D^*}\left(\frac{k_h}{T}\right) \tag{42}$$

Let:

$$K = 6(1-2\mu)\left(\frac{a}{t}\right)^2 * \left([1 + G_2].k_z + \frac{1}{\beta^2}.[1 + G_3].k_{2z}\right) \tag{43}$$

$$A = \frac{(s_{12}s_{23} - s_{13}s_{22})}{(s_{12}s_{12} - s_{11}s_{22})} \tag{44}$$

$$B = \frac{(s_{12}s_{13} - s_{11}s_{23})}{(s_{12}s_{12} - s_{11}s_{22})} \tag{45}$$

Where:

$$s_{11} = (1-\mu)k_x + \frac{1}{2\beta^2}(1-2\mu)k_{xy} + 6(1-2\mu)\left(\frac{a}{t}\right)^2 k_z \tag{46}$$

$$s_{22} = \frac{(1-\mu)}{\beta^4}k_y + \frac{1}{2\beta^2}(1-2\mu)k_{xy} + \frac{6}{\beta^2}(1-2\mu)\left(\frac{a}{t}\right)^2 k_{2z} \tag{47}$$

$$s_{23} = s_{32} = -\frac{6}{\beta^2}(1-2\mu)\left(\frac{a}{t}\right)^2 k_{2z} \tag{48}$$

$$s_{13} = -6(1-2\mu)\left(\frac{a}{t}\right)^2 k_z \tag{49}$$

$$s_{12} = s_{21} = \frac{1}{2\beta^2}k_{xy} \tag{50}$$

$$D^* = \frac{Et^3}{12(1+\mu)(1-2\mu)} \tag{51}$$

D^* denotes the modulus of rigidity of 3-D plate.

2.4. Numerical Analysis

The analysis of an isotropic thick rectangular plate whose Poisson's ratio is 0.3, carrying uniformly distributed load (including self-weight) and subjected to CCCS plate boundary condition shown in Figure 1 for at varying span to depth and aspect ratios of the plate is presented in this section.

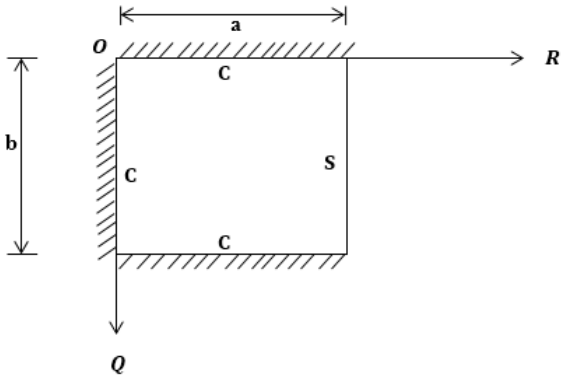

Figure 1: CCCS rectangular plate

The plate in Figure 1 has the following initial conditions:

$$\text{At } R = Q = 0; \text{deflection } (w) = 0 \tag{52}$$

$$\text{At } R = Q = 0; \text{ slope } \left(\frac{dw}{dR} and \frac{dw}{dQ}\right) = 0 \tag{53}$$

$$\text{At } R = Q = 1; \text{deflection } (w) = 0 \tag{54}$$

$$\text{At } R = Q = 1, \text{bending moment} \left(\frac{d^2w}{dR^2}\right) = 0; \text{ Q } = 1, \text{ slope } \left(\frac{dw}{dQ}\right) = 0 \tag{55}$$

By substituting the boundary conditions in Equation (33) to (36) into the derived function of deflection in Equation (22) in line with the work of Onyeka *et al.* (2022a), the particular solution of the deflection is obtained as:

$$w = a_3 \times b_2 (g_1 - g_1 R - g_1 Cos\, g_1 R + Sin\, g_1 R).(Cos2\pi Q - 1) \tag{56}$$

Let,

$$C_1 = a_3 \times b_2 \tag{57}$$

and;

$$h = (g_1 - g_1 R - g_1 Cos\, g_1 R + Sin\, g_1 R).(Cos2\pi Q - 1) \tag{58}$$

Thus:

$$w = C_1 (g_1 - g_1 R - g_1 Cos\, g_1 R + Sin\, g_1 R).(Cos2\pi Q - 1) \tag{59}$$

Where w and h are deflection and shape function of the plate respectively.

2.5. Exact Displacement and Stress Expression

The expression for the in-plane displacement (u *and* v), deflection (w) and stress of 3-D plate were derived by substituting the values of C_1, C_2 *and* C_3 in Equation (49), (38) and (39) into Equation (12) – (17), simplify appropriately gives:

$$u = \text{z}.\frac{C_2}{a}.\frac{\partial h}{\partial Q} \tag{60}$$

$$w = C_1 (g_1 - g_1 R - g_1 Cos\, g_1 R + Sin\, g_1 R).(Cos2\pi Q - 1) \tag{61}$$

$$\sigma_x = \frac{\text{Ets}}{(1+\mu)(1-2\mu)\text{a}}\left[C_2 \frac{\partial^2 h}{\partial R^2} + \mu\, \frac{C_3}{\beta^2}\, \frac{d^2 h}{dQ^2} + \frac{(1-\mu)\text{a}}{\text{st}^2}.\frac{\partial \text{w}}{\partial \text{S}} \right] \tag{62}$$

$$\sigma_y = \frac{Ets}{(1+\mu)(1-2\mu)a}\left[\mu . C_2 \frac{\partial^2 h}{\partial R^2} + (1-\mu).\frac{C_3}{\beta^2}\frac{d^2 h}{dQ^2} + \frac{\mu a}{st^2}.\frac{\partial w}{\partial S}\right] \quad (63)$$

$$\sigma_z = \frac{Ets}{(1+\mu)(1-2\mu)a}\left[\frac{\mu}{C_2}.\frac{\partial^2 h}{\partial R^2} + \mu\ \frac{C_3}{\beta}\frac{\partial^2 h}{\partial Q^2} + \frac{(1-\mu)a}{st^2}.C_1.\frac{\partial \mathrm{h}}{\mathrm{a}\,\partial \mathrm{t}}\right] \quad (64)$$

$$\tau_{xy} = \frac{\mathrm{Ets}}{2(1+\mu)(1-2\mu)}.\frac{1}{\beta a^3}[\,C_2 + C_3]\frac{\partial^2 h}{\partial R\,\partial Q} \quad (65)$$

$$\tau_{yz} = \frac{\mathrm{Ets}}{2(1+\mu)(1-2\mu)}.\frac{1}{\beta a^2}\left[\,C_1 + \frac{C_3}{t}.\frac{\partial z}{\mathrm{a}\,\partial t}\right]\frac{\partial h}{\partial Q} \quad (66)$$

$$\tau_{xz} = \frac{E(1-2\mu)ts}{2(1+\mu)(1-2\mu)a}.\left[\frac{a}{ts}\theta_x + \frac{1}{ts}C_1.\frac{\partial \mathrm{h}}{\mathrm{a}\,\partial \mathrm{t}}\right] \quad (67)$$

3. RESULTS AND DISCUSSION

Table 1 and 2 show the result of the non-dimensional value of displacements and stresses at different span-thickness aspect ratio in a rectangular thick plate aspect ratio of 1 and 2 respectively. After substituting Equation 58 into Equations (30), (31), (32), (33), (34) and (35), the numerical k-values (k_1, k_2, k_3, k_4, k_5 and k_h) for CCCS supported rectangular plate is obtained as presented in the Figure 2. This k-values were used to obtain the value of the shape functions and displacement and rotation of the plate material when subjected to a uniformly distributed transverse load under the same boundary conditions.

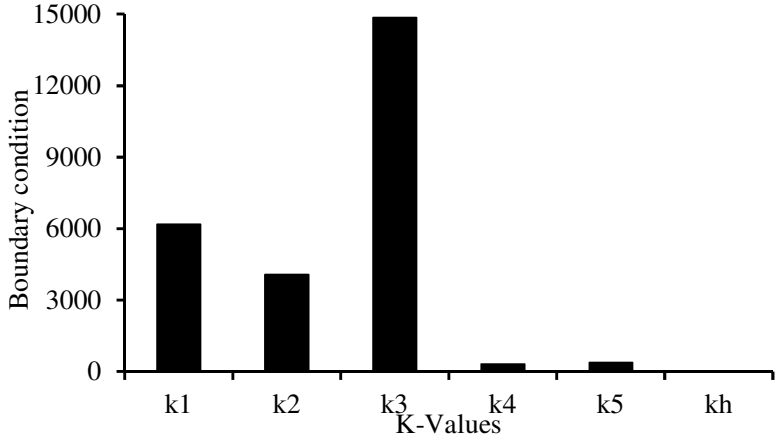

Figure 2: K-values for the CCCS plate boundary condition

Tables 1 and 2 contains the numerical representation of the result of the non-dimensional displacements (u, v & w) and the stresses characteristics of a CCCS rectangular plate using the established exact trigonometric displacement function. The numerical comparison presented in Table 3 was made to show the disparities between the present study and the literature under review to show the effect of aspect ratio on the 3-D bending and stress analysis of rectangular plate at varying thickness. The span to thickness ratio considered were 4, 5, 10, 15, 20, 50, 100 and CPT, which is obviously seen to span from the thick plate, moderately thick plate and thin plate (Onyeka and Edozie, 2020). The present work obtained non-dimensional result of displacement and stresses of the plate by expressing the deflection and rotation functions of the plate in the form of trigonometry to analyze the effect of aspect ratio of the bending characteristics of the plate.

Table 1: The result of displacements and stresses of a CCCS plate aspect ratio of 1

$\beta = \frac{a}{t}$	w	u	v	σ_x	σ_y	σ_z	τ_{xy}	τ_{xz}	τ_{yz}
4	0.00321	-0.00097	-0.00305	0.23451	0.25799	0.24497	-0.02686	0.00408	0.01681
5	0.00301	-0.00094	-0.00303	0.23065	0.25579	0.22855	-0.02647	0.00312	0.01314
10	0.00209	-0.00067	-0.00242	0.17952	0.20560	0.20704	-0.02034	0.00084	0.00320
15	0.00194	-0.00062	-0.00232	0.17091	0.19746	0.20310	-0.01933	0.00049	0.00153
20	0.00189	-0.00060	-0.00229	0.16795	0.19469	0.20172	-0.01898	0.00039	0.00095
50	0.00184	-0.00059	-0.00226	0.16478	0.19174	0.20024	-0.01860	0.00024	0.00034
100	0.00183	-0.00058	-0.00225	0.16433	0.19132	0.20003	-0.01855	0.00023	0.00025
CPT	0.00183	-0.00058	-0.00225	0.16418	0.19118	0.20003	-0.01853	0.00022	0.00022

The non-dimensional result in the Tables 1 shows that as the span-thickness ratio of the plate increased, the in-plane displacement and deflection (w) characteristics which occurs at the plate due to the applied load decreased. On the other hand, the stress perpendicular to the x, y and z axis ($\sigma_x,\ \sigma_y$ & σ_z) decreased as the span-depth ratio of the plate increases. Meanwhile, the increase at the span-thickness ratio of the plate increases the value shear stress along the x-y (τ_{xy}) while the span - depth ratio causes a decrease in the value shear stress along the x-z and y-z plane (τ_{xz} & τ_{yz}). These decrease continue until failure occurs in the plate structure. This is quite expected considering the established theory of structures because when load is applied to a structural member with a less thickness, more stresses are induced and the structure bend to resist the load thereby causing deflection of the material to increase. When the deflection increase beyond the elastic limit of the very material, failure abounds.

Table 1 shows that, at a span-thickness ratio between 4 and 20, the value of deflection (w) of the plate varied between 0.0032 and 0.0018. These values maintain a constant value of 0.0018 at the span - thickness 20 till 100 which is equal to the value of the CPT. It was observed that the value of deflection is more for a thicker plate than thinner plate under the same loading capacity/condition. This deflection becomes constant and equal to the value of the CPT at span-thickness ratio of 20 and above under the same loading capacity/condition. These decrease continue until the plate structure deflects beyond the elastic yield stress, hence, failure occurs.

Table 2: The result of displacements and stresses of a CCCS plate aspect ratio of 2

$\beta = \frac{a}{t}$	w	u	v	σ_x	σ_y	σ_z	τ_{xy}	τ_{xz}	τ_{yz}
4	0.00784	-0.00288	-0.00462	0.49370	0.28724	0.24079	-0.0381	0.00918	0.01297
5	0.00676	-0.00261	-0.00418	0.44689	0.26211	0.22437	-0.0346	0.00572	0.00801
10	0.00545	-0.00229	-0.00365	0.39560	0.23159	0.20286	-0.0303	0.00152	0.00249
15	0.00522	-0.00224	-0.00356	0.38670	0.22627	0.19892	-0.0295	0.00079	0.00205
20	0.00514	-0.00222	-0.00352	0.38362	0.22443	0.19754	-0.0292	0.00054	0.00103
50	0.00506	-0.00220	-0.00349	0.38033	0.22246	0.19606	-0.0290	0.00027	0.00029
100	0.00505	-0.00219	-0.00349	0.37986	0.22218	0.19585	-0.0289	0.00023	0.00024
CPT	0.00504	-0.00219	-0.00348	0.37970	0.22208	0.19585	-0.0289	0.00022	0.00022

Similarly, the non-dimensional result in the Tables 2 shows that as the span-thickness ratio of the plate increased, the in-plane displacement and deflection (w) characteristics which occurs at the plate due to the applied load decreased. On the other hand, the stress perpendicular to the x, y and z axis ($\sigma_x,\ \sigma_y$ & σ_z) decreases as the span-depth ratio of the plate increased. Meanwhile, the increase of the span-thickness ratio of the plate resulted to an increase in the value shear stress along the x-y (τ_{xy}) while the span-depth ratio caused a decrease in the value shear stress along the x-z and y-z plane (τ_{xz} & τ_{yz}). This trend continued until failure occurs in the plate structure.

Table 2 shows that, at a span-thickness ratio between 4 and 20, the value of the deflection (w) of the plate varied between 0.0078 and 0.0051. These values maintain a constant value of 0.0051 at the span - thickness 20 till 100 which is equal to the value of the CPT. It is discovered that the value of deflection varies more as the plate is thicker and vary less as the span to thickness increase (thinner plate) under the same loading capacity/condition. This deflection becomes constant and equal to the value of the CPT at span-thickness

ratio of 20 and above under the same loading capacity/condition. These decrease continue until the plate structure deflects beyond the elastic yield stress, hence, failure occurs.

Study in the Table 1 and 2 shows that as the aspect ratio of the plate increase, the in-plane and out-of-plane displacement characteristics (u and v) decrease whereas, the deflection (w) which occurs in the plate due to the applied load increase with increases in the value of the span-thickness ratio of the plate. On the other hand, the stress perpendicular to the x, y and z axis ($\sigma_x,\ \sigma_y$ & σ_z) increases as the span-depth ratio of the plate increases. This implies that, as the length of the plate material increases, more stresses are induced in the plate which consequently leads to the failure of the plate material if the plate material are stretched beyond the elastic limit. This means that the failure in a plate structure is bound to occur as the more stresses are induced within the plate element which affects the performance in terms of the serviceability of the plate. Thus, caution must be taken when selecting the depth and other dimensions along the x and y co-ordinate of the plate to ensure safety and accuracy of the analysis.

In summary, there are three categories of rectangular plates. The plates whose deflection and vertical shear stress do not vary well from zero will be classified as thin plates because its value is almost equal to the value of the CPT. Hence, the plate whose deflection and transverse shear stress varies very much from zero is categorized as thick plates. Thus, the span-thickness ratio for these categories of rectangular plates are: Thick plate is categorized as the plate with the span to thickness ratio: $a/t \leq 20$ while the thin plate is categorized as the plate with the span to thickness ratio: $a/t \geq 100$. Meanwhile, the present theory stress prediction shows that the result of the displacement and stress of thin and moderately thick plate using the 3-D theory is the same for the bending analysis of rectangular plate under the CCCS boundary condition.

The comparative analysis performed as presented in the Table 3 showed that the plate with the largest thickness (a/t of 4) gave a percentage difference of 7.32%, 19% and 14.7% compared with Onyeka and Edozie (2020), Ezeh *et al.* (2018) and Li *et al.* (2015) respectively. On the other hand, the thinnest plate (a/t of 100 and above) gives a percentage difference of 12.5% and 12.1% of the work of Onyeka and Edozie (2020) and Ezeh *et al.* (2018) respectively, when compared with the present study. However, the percentage difference between the present study and the three past works in consideration, decreases and its value get closer as the plate is getting thinner. Meanwhile, that the overall average percentage difference values of deflection for present theory and those of Onyeka and Edozie (2020) and Ezeh *et al.* (2018) is 6.7% and 8.6% respectively. The small difference (6.7%) between the present study and that of Onyeka and Edozie (2020) is quite expected as both authors used a derived shape function in the analysis, unlike Ezeh *et al.* (2018) which used an assumed shape function. Despite the fact that both Onyeka and Edozie (2020), and Ezeh *et al.* (2018) used a third order RPT their work differs more when compared with the present study. This shows that derived shape function, enhanced close form solution in plate analysis.

Table 3: Comparative deflection analysis for square plate between present study and past studies showing their percentage difference calculations at varying span-thickness ratio (β = a/t)

$\beta = \frac{a}{t}$	Present work	Onyeka and Edozie (2020)	% Diff.	Ezeh *et al.* (2018)	% Diff.	Li *et al.* (2015)	% Diff.
5	0.3006	0.2786	7.32	0.2434	19.0	0.2565	14.7
10	0.2094	0.1874	10.5	0.1816	13.3	0.1833	12.5
20	0.1892	0.1672	11.6	0.1660	12.3	0.1660	12.3
50	0.1837	0.1617	11.9	0.1615	12.1	-	-
100	0.183	0.1601	12.5	0.1609	12.1	-	-
5	0.3006	0.2786	7.32	0.2434	19.0	0.2565	14.7
Average % diff.		6.7		8.6		4.9	
Av. total % diff.				6.8			

Thus, the present model using a derived shape function is shown to be more reliable to use as it considered the six stress elements to yield the exact solution for the analysis of thick plate that is clamped supported at

the first-three edges and other one edge simply supported (CCCS). Hence, the result of the present analysis, which contains all the stress element and ensured that the variation of the stresses through the thickness of the plate which induced buckling are uniformly distributed, showed that the present method can be used with confidence for bending analysis of plate.

4. CONCLUSION

The 3-D bending and stress analysis of thick rectangular plate using 3-D elasticity theory has been investigated. From the study, the following conclusion has been drawn:

i. It is concluded that the present theory stress prediction shows that the result of the displacement and stress of thin and moderately thick plate using the 3-D theory is the same for the bending analysis of rectangular plate under the CCSS boundary condition.

ii. Plate analysis required 3-D analogy for a true solution, but the 2-D shear deformation theory gives an unrealistic solution.

iii. The 3-D exact plate model developed in this study are variationally consistent and can be used in the analysis of any category of plate.

5. CONFLICT OF INTEREST

There is no conflict of interest associated with this work.

REFERENCES

Chandrashekhara, K. (2001). *Theory of Plates*. University Press (India) Limited.

Ezeh, J. C., Ibearugbulem, O. M., Ettu, L. O., Gwarah, L. S. and Onyechere, I. C. (2018). Application of Shear Deformation Theory for Analysis of CCCS and SSFS Rectangular Isotropic Thick Plates. *IOSR Journal of Mechanical and Civil Engineering (IOSR-JMCE)*, *15*(5), pp. 33-42.

Grigorenko, A. Y. Bergulev, A. S. and Yaremchenko, S.N. (2013). Numerical solution of bending problems for rectangular plates," *International Applied Mechanics,* 49(1), pp. 81-94.

Gujar, P. S. and Ladhane, K. B. (2015). Bending analysis of simply supported and clamped circular plate. *International Journal of Civil Engineering (SSRG-IJCE)*, 2(5), pp. 45-51.

Ibearugbulem, O. M. Ezeh, J. C. Ettu, L. O. Gwarah, L. S. (2018). Bending Analysis of Rectangular Thick Plate Using Polynomial Shear Deformation Theory. *IOSR Journal of Engineering (IOSRJEN)*, 8(9), pp. 53-61.

Ibearugbulem, O. M., Onwuegbuchulem, U. C. and Ibearugbulem, C. N. (2021). Analytical Three-Dimensional Bending Analyses of Simply Supported Thick Rectangular Plate. *International Journal of Engineering Advanced Research, 3*(1), pp. 27-45.

Ike, C. C. (2017). Kantorovich-Euler Lagrange-Galerkin's Method for Bending Analysis of Thin Plates," *Nigerian Journal of Technology (NIJOTECH),* 36(2), pp. 351-360.

Kirchhoff, G. R. (1850). "U''ber Das Gleichgewicht and Die Bewe Gung Einer Elastschen Scheibe. *Journal f'' Ur Die Reine Und Angewandte Mathematik*, 40, pp. 51-88.

Li, R., Wang, P., Tian, Y., Wang, B. and Li, G. (2015). A Unified Analytic Solution Approach to Static Bending and Free Vibration Problems of Rectangular Thin Plates. *Scientific Reports, 5*, pp. 17-54.

Mama, B. O. Nwoji, C. U. Ike, C. C. and Onah, H. N. (2017). Analysis of simply supported rectangular Kirchhoff plates by the finite Fourier sine transform method. *International Journal of Advanced Engineering Research and Science,* 4(3), pp. 285-291.

Mindlin, R. D. (1951). Influence of Rotatory Inertia and Shear on Flexural Motions of Isotropic, Elastic Plates. *Journal of Applied Mechanics,* 18(1), pp. 31-38.

Nwoji, C. U. Onah, H. N. Mama, B. O. and Ike, C. C. (2018). Ritz variational method for bending of rectangular Kirchhoff plate under transverse hydrostatic load. *Mathematical Modelling of Engineering Problems*, 5(1), pp. 1-10.

Onyeka, F. C. (2020). Critical Lateral Load Analysis of Rectangular Plate Considering Shear Deformation Effect. *Global Journal of Civil Engineering*, 1, pp. 16–27.

Onyeka, F. C. (2021). Effect of Stress and Load Distribution Analysis on an Isotropic Rectangular Plate. *Arid Zone Journal of Engineering, Technology & Environment*, 17(1), pp. 9-26.

Onyeka, F. C. and Ibearugbulem, O. M. (2020). Load Analysis and Bending Solutions of Rectangular Thick Plate. *International Journal on Emerging Technologies*, *11*(3), pp. 1103-1110.

Onyeka, F. C. and Mama, B. O. (2021). Analytical Study of Bending Characteristics of an Elastic Rectangular Plate using Direct Variational Energy Approach with Trigonometric Function. *Emerging Science Journal*, 5(6), pp. 916-928.

Onyeka, F.C. and Edozie, O. T. (2020). Application of Higher Order Shear Deformation Theory in the Analysis of thick Rectangular Plate. *International Journal on Emerging Technologies, 11*(5), pp. 62–67.

Onyeka, F. C. and Okeke, T. E. (2021a). Analytical Solution of Thick Rectangular Plate with Clamped and Free Support Boundary Condition using Polynomial Shear Deformation Theory. *Advances in Science, Technology and Engineering Systems Journal*, 6(1), pp. 1427-1439.

Onyeka, F. C. and Okeke, T. E. (2021b). Analysis of critical imposed load of plate using variational calculus. *Journal of Advances in Science and Engineering*, *4*(1), pp. 13-23.

Onyeka, F. C. and Okeke, T. E. (2021c). New refined shear deformation theory effect on non-linear analysis of a thick plate using energy method. *Arid Zone Journal of Engineering, Technology and Environment*, 17(2), pp. 121-140.

Onyeka, F. C. and Okeke, T. E. (2021d). Elastic Bending Analysis Exact Solution of Plate using Alternative I Refined Plate Theory. *Nigerian Journal of Technology (NIJOTECH)*, 40(6), pp. 1018-1029.

Onyeka, F. C., Mama, B. O. and Nwa-David, C. D. (2022). Application of variation method in three dimensional stability analysis of rectangular plate using various exact shape functions. *Nigerian Journal of Technology*, *41*(1), pp. 8-20.

Onyeka, F. C., Okafor, F. O. and Onah, H. N. (2021a). Buckling Solution of a Three-Dimensional Clamped Rectangular Thick Plate Using Direct Variational Method. *IOSR Journal of Mechanical and Civil Engineering (IOSR-JMCE)*, 18(3), pp.10-22.

Onyeka, F. C., Okafor, F. O. and Onah, H. N. (2021b). Application of a New Trigonometric Theory in the Buckling Analysis of Three-Dimensional Thick Plate. *International Journal of Emerging Technologies*, *12*(1), pp. 228-240.

Onyeka, F. C., Nwa-David, C. D. and Arinze, E. E. (2021c). Structural Imposed Load Analysis of Isotropic Rectangular Plate Carrying a Uniformly Distributed Load Using Refined Shear Plate Theory. *FUOYE Journal of Engineering and Technology (FUOYEJET)*, 6(4), pp. 414-419.

Onyeka, F. C., Okeke, T. E. and Nwa-David, C. D. (2022a). Buckling Analysis of a Three-Dimensional Rectangular Plates Material Based on Exact Trigonometric Theory. *Journal of Engineering Research and Sciences*, 1(3), pp. 106-115.

Onyeka, F. C., Mama, B. O. and Okeke, T. E. (2022b). Exact Three-Dimensional Stability Analysis of Plate Using a Direct Variational Energy Method. *Civil Engineering Journal*, 8(1), pp. 60–80.

Onyeka, F. C., Mama, B. O. and Nwa-David, C. D. (2022c). Analytical Modelling of a Three-Dimensional (3D) Rectangular Plate Using the Exact Solution Approach. *IOSR Journal of Mechanical and Civil Engineering (IOSR-JMCE),* 11(1), pp. 10-22.

Onyeka, F. C., Osegbowa, D. and Arinze, E. E. (2021d). Application of a New Refined Shear Deformation Theory for the Analysis of Thick Rectangular Plates. *Nigerian Research Journal of Engineering and Environmental Sciences,* 5(2), pp. 901-917.

Osadebe, N. N. Ike, C. C. Onah, H. N. Nwoji, C. U. and Okafor, F. O. (2016). Application of the Galerkin-Vlasov Method to the Flexural Analysis of Simply Supported Rectangular Kirchhoff Plates under Uniform Loads. *Nigerian Journal of Technology*, 35(4), pp. 732.

Reddy, J. N. (2006). *Theory and Analysis of Elastic Plates and Shells*. CRC press.

Reissner, E. (1945). The Effect of Transverse Shear Deformation on the Bending of Elastic Plates. *Journal of Applied Mechanics,* 12(2), pp. A69–A77.

Sayyad, I. I. (2013). Bending and Free Vibration Analysis of Isotropic Plate Using Refined Plate Theory. *Bonfring International Journal of Industrial Engineering and Management Science*, 3(2), pp. 40-46.

Sayyad, A. S. and Ghugal, Y. M. (2012). Bending and free vibration analysis of thick isotropic plates by using exponential shear deformation theory. *Applied and Computational Mechanics,* 6, pp. 65-82.